Journal of Electrical Engineering and Computer (JEECOM)
Vol. 8, No. 1 (2026), DOI: 10.33650/jeecom.v4i2
p-ISSN: 2715-0410; e-ISSN: 2715-6427

Multi-Channel Power Data Acquisition System for Solar Panel Monitoring

Septia Refly *[1], Adam Bimajaya [2], Basyaruddin Ismail Harahap [3]
[1,2,3] Electrical Engineering, Universitas Maritim Raja Ali Haji, Tanjungpinang, Indonesia

Article Info

Article history:

Received January 19, 2026
Revised January 26, 2026
Accepted March 6, 2026

Keywords:

Solar panel
Monitoring
Data acquisition
INA219 sensor
ThingSpeak

ABSTRACT

This study presents a low-cost and scalable multi-channel power data acquisition system for real-time solar photovoltaic (PV) panel monitoring, addressing the limitations of conventional single-channel approaches that provide only aggregate system measurements. The proposed system enables simultaneous per-panel measurement to support detailed performance analysis and improved fault localization. The system is implemented using an ESP32 microcontroller integrated with multiple calibrated INA219 sensors, which are connected via the I²C protocol to measure voltage, current, and electric power. A modular hardware design supports three independent PV channels, while data handling is achieved through dual-mode operation, consisting of local microSD card storage and wireless data transmission to the ThingSpeak IoT platform for real-time visualization. Calibration results demonstrate high measurement accuracy, with average errors below 1%, a voltage root mean square error (RMSE) of less than 0.07 V, and a current RMSE of less than 7 mA. Field testing conducted over two consecutive days confirms stable and uninterrupted operation, achieving 100% data acquisition reliability. The recorded data clearly reveal per-panel performance differences under real operating conditions, enabling effective identification of mismatch behavior among panels. The proposed system provides an affordable, reliable, and scalable solution for distributed PV monitoring, making it suitable for multi-panel and remote photovoltaic installations. Future improvements will involve temperature-based efficiency analysis and the integration of thermal management strategies to enhance photovoltaic performance.

Corresponding Author:
Septia Refly,
Universitas Maritim Raja Ali Haji,
Jl. Raya Dompak, Dompak, Tanjungpinang 29111, Indonesia
Email: septiarefly@umrah.ac.id

1. INTRODUCTION

The increasing global demand for clean and renewable energy has positioned solar photovoltaic (PV) systems as a leading alternative to conventional energy sources [1,2]. As solar power installations become more widespread, the need for reliable, accurate, and cost-effective monitoring systems becomes increasingly critical to ensure optimal performance and longevity of PV infrastructures [3]. Effective monitoring not only facilitates real-time tracking of energy production but also enables early detection of faults, degradation, and operational inefficiencies [4]. Such real-time tracking capabilities are commonly achieved using Internet of Things (IoT) technology. Among various IoT data visualization platforms, ThingSpeak—an IoT analytics service developed by MathWorks—remains a popular choice due to its ease of use, open-source accessibility, and extensibility for data visualization and analysis [5][6].

Despite these advancements in IoT platforms, a gap remains in the data acquisition layer. Most conventional low-cost PV monitoring systems rely on centralized, single-channel data acquisition units that measure only the aggregate output of an entire PV array [7], [8]. Such single-channel architectures lack the granularity required to capture per-panel performance variations, making it difficult to identify mismatch faults such as partial shading or individual panel degradation within a PV string. Furthermore, several existing studies

have focused on monitoring a single PV module rather than multi-panel configurations [9], [10], [11]. Although commercial multi-channel monitoring solutions are available, they often lack the cost-effectiveness and open scalability necessary for widespread deployment in remote or off-grid environments.

To achieve for cost-effective precision, several recent studies have explored the use of the INA219 sensor for power monitoring applications due to its precision, compact form factor, low power consumption, and compatibility with I²C-based microcontroller platforms. Prasetyawati et al. [12] demonstrated that INA219, properly calibrated and validated, can achieve accuracies exceeding 99% in both voltage and current measurements. Furthermore, Muqorrobin et al. [13] utilized INA219 in a remote solar monitoring system using an ESP32 and Handy Talkie (HT) communication, which achieved low error rates and demonstrated its effectiveness in real-world off-grid conditions These studies confirm the suitability of INA219 for distributed PV monitoring systems where affordability and scalability are essential. However, most existing implementations employ the sensor in single-node configurations, leaving the potential of a scalable and synchronized multi-channel architecture largely unexplored.

To address these limitations, this study proposes the design and implementation of a low-cost multi-channel power data acquisition system for solar panel monitoring. The proposed system enables simultaneous per-panel measurement of voltage, current, and power, thereby enhancing fault localization and performance analysis. The system is implemented on three solar panels using calibrated INA219 sensors to ensure reliable data acquisition. Measured power data are transmitted and visualized in real time via the ThingSpeak IoT platform. By combining a microcontroller-based hardware architecture with a flexible data acquisition scheme, the proposed system offers an affordable and scalable solution for multi-panel photovoltaic monitoring applications.

2. METHOD

The experimental study was carried out at the Renewable Energy Laboratory, Universitas Maritim Raja Ali Haji, between 08:00 and 16:00 WIB. Data were recorded at one-minute intervals and visualized through the ThingSpeak IoT platform to evaluate time-based variations. The primary components of the developed power data acquisition system as shown in Figure 1 consist of input, process and output. The ESP32 serves as the central processing unit, offering dual-core performance, integrated Wi-Fi and Bluetooth connectivity, and support for both I²C and SPI communication protocols [14]. The INA219 sensors, connected via the I²C interface, provide accurate measurements of voltage and current up to 26 V and 3.2 A, respectively [15]. The DS3231 RTC module maintains time synchronization and preserves timestamp accuracy during power loss through its battery backup feature [16]. Measurement data are stored locally via a microSD card adapter interfaced through the SPI protocol, using standard pin configurations compatible with the ESP32. The 3D hardware layout shown in Figure 2. Three polycrystalline solar panels are mounted on a 900 mm x 340 mm x 600 mm frame.

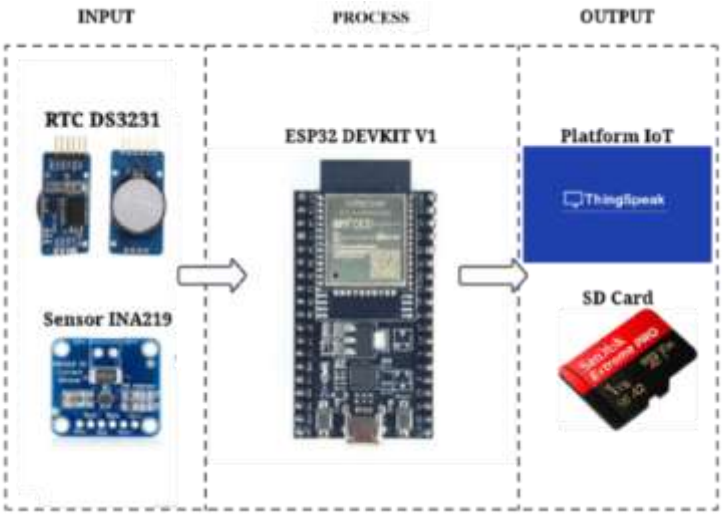

Figure 1. Multi-channel power data acquisition system

ISSN: 2715-6427

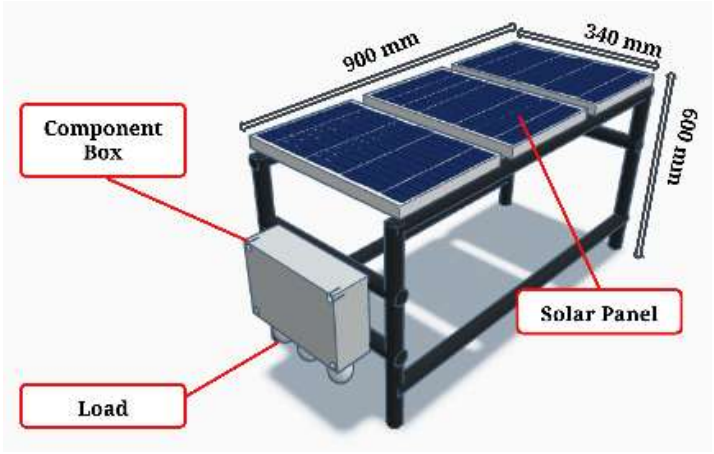

Figure 2. 3D Hardware Design

2.1 System flowchart and schematic design

The operational workflow of the system begins with the initialization and status verification of essential modules, including the INA219 current–voltage sensors, the DS3231 real-time clock (RTC), and the microSD card storage. Once all components are confirmed to be functional, indicated by LED 1 turning on, the ESP32 connects to the internet and synchronizes with the RTC using Network Time Protocol (NTP). The system then enters a monitoring loop that continuously checks whether the current time matches the predefined data acquisition interval. When the condition is met, the ESP32 acquires voltage, current, and power readings from the INA219 sensors. The collected data are simultaneously stored on the microSD card and transmitted to the ThingSpeak cloud platform. If data storage fails, LED 2 is activated to indicate an error. This monitoring cycle continues uninterrupted as long as the system remains powered, enabling reliable real-time tracking of solar panel performance. The diagram depicting the system's operational flow and the complete hardware interconnection schematic are presented in Figure 3 and Figure 4**.**

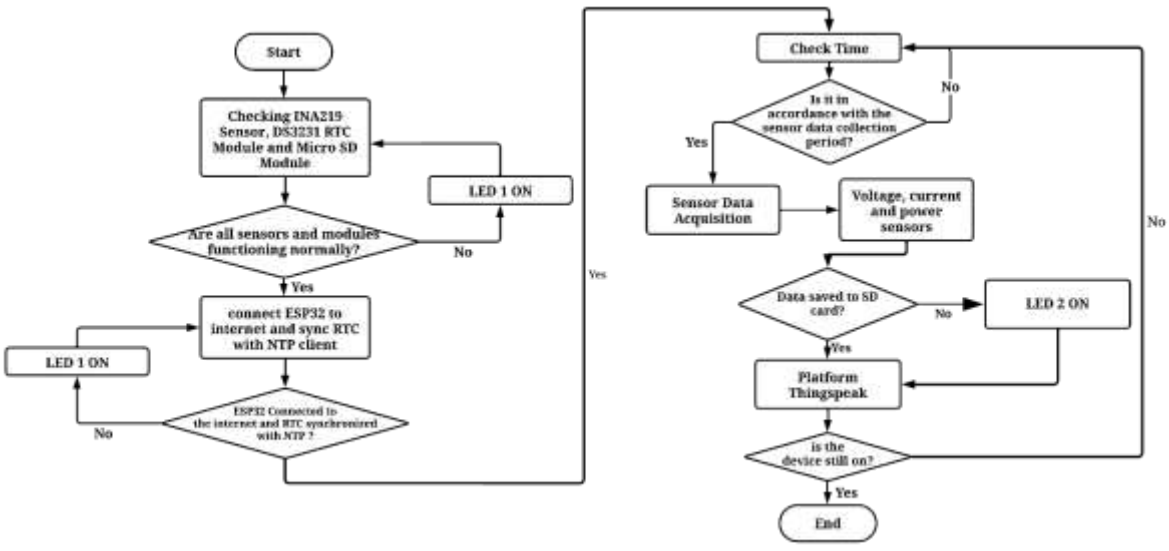

Figure 3. System flowchart

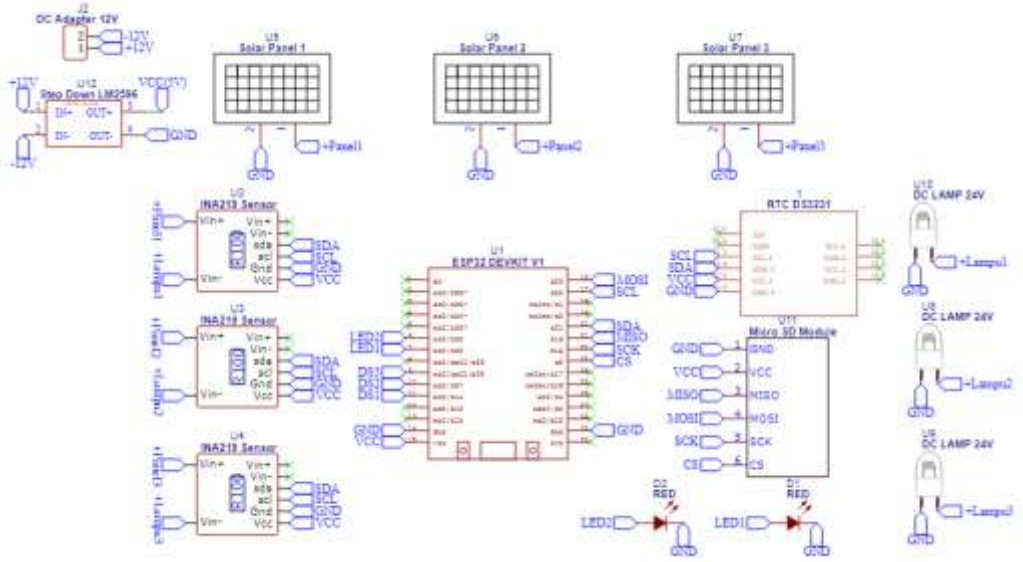

Figure 4. Schematic design of the system

The system is powered by a 12V DC adapter, which is stepped down to 5V using an LM2596 DC-DC buck converter to supply regulated power to the ESP32 microcontroller and peripheral modules. Three solar panels (labeled Panel 1, Panel 2, and Panel 3) are each connected to individual INA219 sensors that measure voltage and current values through I²C communication with the ESP32. The sensors are configured to read power data from each panel independently, enabling multi-channel measurement. The ESP32 module serves as the central processing unit, interfacing with the INA219 sensors via SDA and SCL lines, and controlling the operation of two LEDs (LED1 and LED2) as system status indicators. Real-time timestamping is managed by a DS3231 RTC module, also connected through the I²C interface. Data is stored locally using a microSD card module that communicates with the ESP32 via the SPI protocol, using the standard MOSI, MISO, SCK, and CS pins. Additionally, three 24V DC lamps act as the output loads for each solar panel, simulating real usage conditions. The overall circuit design enables precise per-panel monitoring and real-time data logging for both local storage and cloud-based visualization.

2.2 Calibration sensor

The calibration procedure for the INA219 sensor was divided into two stages: voltage calibration and current calibration. Voltage calibration was performed by comparing the voltage readings from three individual INA219 sensor units against a reference voltage supplied by a programmable power source, within a range of 1 V to 20 V. Each sensor was tested 20 times to ensure data reliability and repeatability. Current calibration, on the other hand, involved comparing the sensor's current readings with reference values obtained from a clamp meter, under load conditions ranging from 80 mA to 1590 mA, with a total of 20 measurement iterations per sensor. The corresponding formulations used to assess the sensor's performance include the absolute error, error percentage, and accuracy percentage, as presented in Equation (1), (2), and (3) [17].

$$error = Calibrator\ Value - Sensor\ Value \quad (1)$$

$$Error\ percentage = \frac{error}{Calibrator\ Value} \times 100\% \quad (2)$$

$$Accuracy\ Percentage = 100\% - Error\ percentage \quad (3)$$

In addition to the basic error metrics, the Root Mean Square Error (RMSE) in equation (4) was calculated to quantify the overall deviation between the sensor readings (y_a) and the reference values (y_b), providing a comprehensive measure of measurement accuracy. A linear regression analysis was also performed to obtain a calibration equation that defines the relationship between the sensor output and the corresponding reference values, allowing for systematic correction of measurement deviations. y in Equation (5) is the dependent variable, a is intercept, X is independent variable and b is coefficient of variable X. To assess the goodness of fit, the coefficient of determination (R^2) in equation (6) was determined, representing the proportion of variance in the reference data that can be explained by the sensor measurements [18]. n in

ISSN: 2715-6427

equation (4) and (6) represents amount of data, y_i is value of observation, $\hat{y}_i$ is the predicted value and $\bar{y}_i$ is average of all y_i values.

$$\text{RMSE} = \sqrt{\frac{\sum_{i=1}^{n}(y_{b_i} - y_{a_i})^2}{n}} \quad (4)$$

$$y = a + bX \quad (5)$$

$$R^2 = 1 - \frac{SS\ Error}{SS\ Total} = 1 - \frac{\sum_{i=1}^{n}(y_i - \hat{y}_i)}{\sum_{i=1}^{n}(y_i - \bar{y}_i)} \quad (6)$$

3. RESULTS AND DISCUSSION

3.1 Design Result

The system is mounted on a custom-built frame constructed from PVC pipe, designed to support three independent solar panels. Each panel functions as a separate channel within the multi-channel monitoring system, enabling individual power measurement and comparative analysis. At the front of the frame, a component box houses all critical electronic modules, while three 24V DC lamps are mounted below as loads to simulate real energy consumption and complete the system's circuit. Figure 5 presents the physical configuration of the constructed device, whereas Figure 6 depicts the web based interface utilized for data visualization on the ThingSpeak platform.

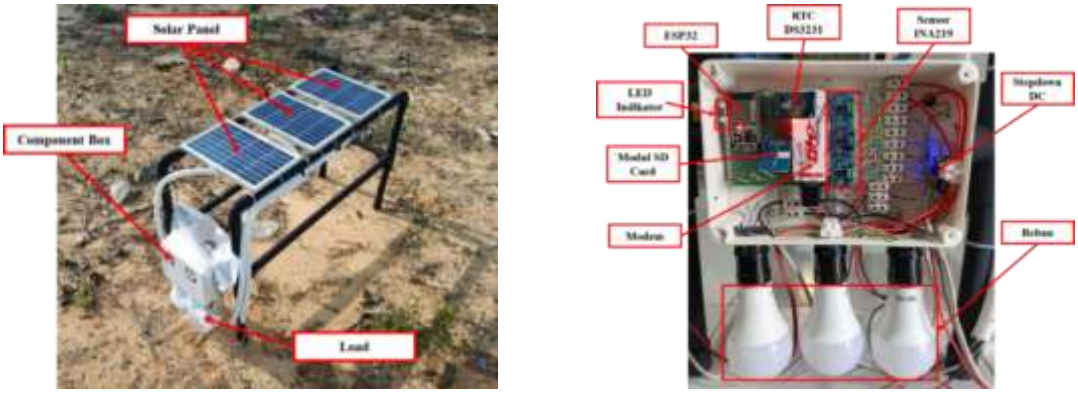

(a) (b)

Figure 5. Physical appearance of the device: (a) The physical setup, (b) Internal view of the component box

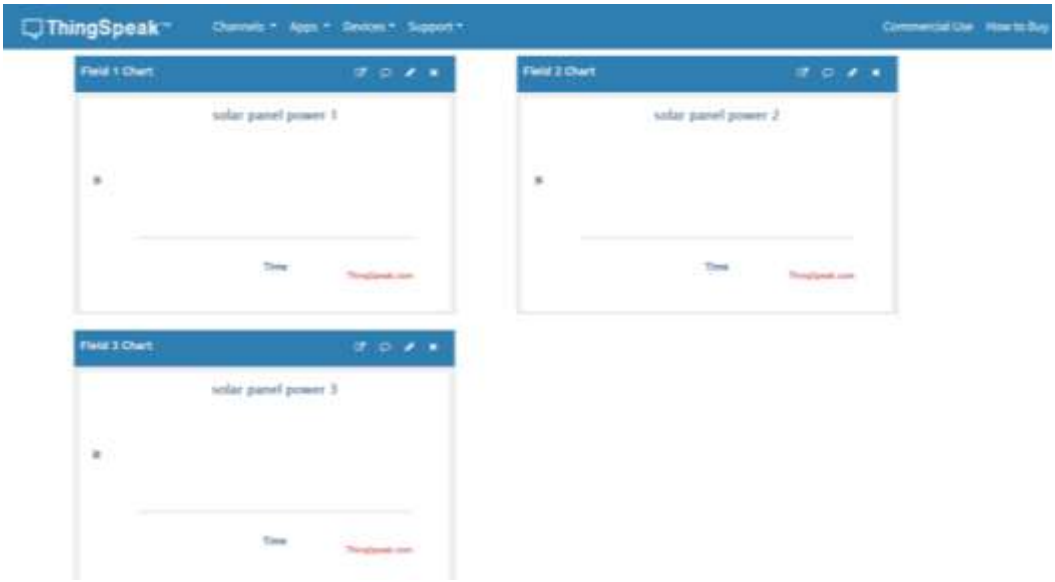

Figure 6. ThingSpeak dashboard web interface

Inside the component box, as shown in Figure 5, the ESP32 microcontroller serves as the central processing unit, interfacing with multiple INA219 sensors for current and voltage measurement. The DS3231 RTC module provides accurate timestamping, while the SD card module allows local data storage. A step-down DC converter regulates the input voltage to 5V to safely power all modules. For real-time data transmission, a modem is integrated to connect the ESP32 to the internet, enabling data uploading to the ThingSpeak IoT platform. Visual status indicators are provided through LED modules, and three 24V DC lamps function as loads for each panel channel. The overall design integrates mechanical stability with electrical functionality, ensuring ease of deployment for field testing and long-duration performance evaluation.

3.2 Calibration Results

3.2.1 Voltage sensor calibration

Each of the three INA219 sensor units was individually tested under identical conditions to assess their accuracy, linearity, and repeatability. The measured sensor values were compared to the corresponding reference voltages, and the results were analyzed through error metrics, regression analysis, and RMSE calculations. The linear relationships obtained from the calibration tests are presented in Figure 7, while a summary of the quantitative calibration outcomes, including average error, error percentage, accuracy percentage, and RMSE is provided in Table 1.

The voltage calibration of the three INA219 sensors demonstrated highly consistent and reliable performance. Each sensor exhibited a strong linear relationship with the reference voltage, as indicated by regression equations with slope values close to one and minimal intercept deviation. The sensors produced low average absolute errors of 0.05 V, with error percentages ranging from 0.37% to 0.43%, indicating minimal deviation from the true values. Accuracy percentages were uniformly high, exceeding 99.5% for all sensors, with Sensor 3 achieving the highest at 99.63%. Furthermore, RMSE values remained below 0.07 V across all units, confirming the precision and stability of the sensors in capturing voltage measurements within the calibrated range.

ISSN: 2715-6427

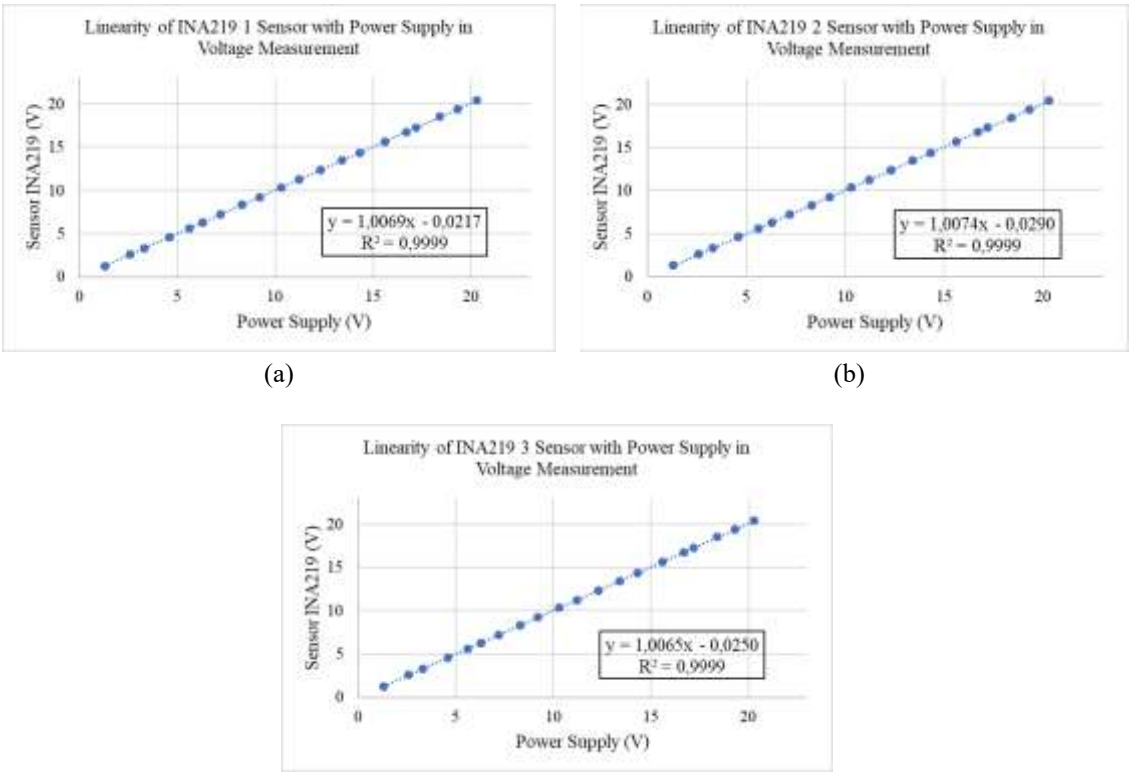

Figure 7. Linearity of INA219 Sensor with power supply reference (a) INA219 Sensor 1, (b) INA219 Sensor 2, and (c) INA219 Sensor 3

Table 1. Summary of voltage calibration results for the three INA219 sensors, including average error, error percentage, accuracy percentage, and RMSE

Sensor	Results			
	Average error	Average percentage error	Average percentage accuracy	RMSE
INA219 sensor 1	0.05 V	0.43 %	99.57 %	0.06709 V
INA219 sensor 2	0.05 V	0.42 %	99.58 %	0.06779 V
INA219 sensor 3	0.05 V	0.37 %	99.63 %	0.06003 V

3.2.2 Current sensor calibration

The output of each sensor was compared to the reference values to analyze linearity and measurement deviation. The linearity of the three sensors during current calibration is illustrated in Figure 8, while the detailed quantitative results, including error, error percentage, accuracy, and RMSE are summarized in Table 2.

The current calibration results of the three INA219 sensors revealed strong linear behavior and acceptable accuracy across the measured range. Each sensor produced regression equations with slopes close to one and R^2 values approaching 1, indicating high consistency and minimal nonlinearity. The average absolute errors ranged from 4.72 mA to 5.62 mA, with error percentages between 0.65% and 1.02%. Accuracy values exceeded 98% for all sensors, with Sensor 3 achieving the highest accuracy at 99.04%. Additionally, RMSE values were all under 7 mA, confirming the reliability and precision of the sensors in current measurement applications.

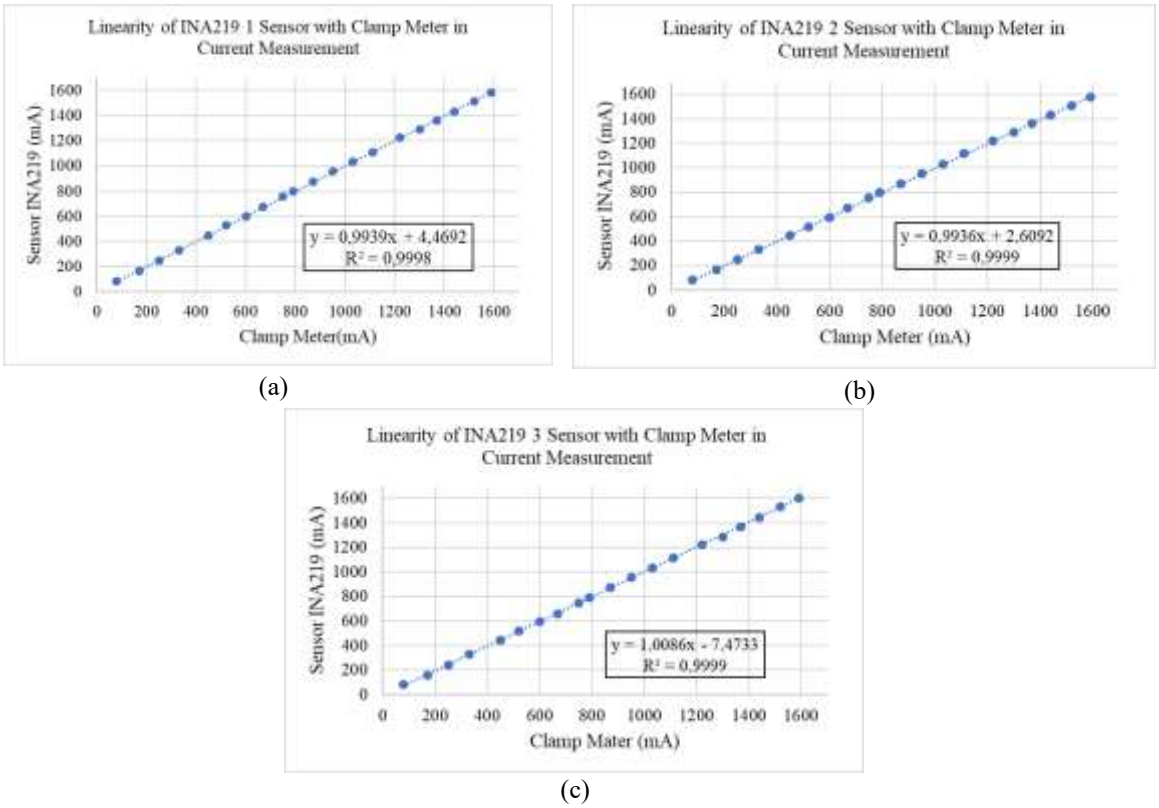

Figure 8. Linearity of INA219 Sensor with clamp meter reference: (a) INA219 Sensor 1, (b) INA219 Sensor 2 and (c) INA219 Sensor 3

Table 2. Summary of current calibration results for the three INA219 sensors, including average error, error percentage, accuracy percentage, and RMSE

Sensor	Results			
	Average error	Average percentage error	Average percentage accuracy	RMSE
INA219 sensor 1	5.62 mA	1.02 %	98.98 %	6.3893 mA
INA219 sensor 2	4.72 mA	0.65 %	99.35 %	6.1144 mA
INA219 sensor 3	5.47 mA	0.96 %	99.04 %	6.7786 mA

3.3 System Performance

The operational stability and real-time monitoring capability of the developed multi-channel acquisition system were evaluated through two consecutive 8-hour tests conducted under field conditions. Both tests took place from 08:00 to 16:00 WIB and successfully generated 481 complete data points each, without any data loss, demonstrating high system reliability in both wireless transmission and local data storage

3.3.1 Day one

On the first day, the test was conducted under relatively stable weather conditions. All three solar panels showed a gradual increase in power output during the morning, reaching a peak between 14:00 and 15:00 WIB, and then steadily declined toward late afternoon. Solar Panel 2 consistently delivered the highest output, while Panels 1 and 3 exhibited similar performance with slight variations. Power readings ranged from approximately 0.2 W to 1.3 W, indicating smooth irradiance changes throughout the day. These findings validate the system's ability to monitor individual panel performance and capture diurnal variations accurately and continuously, as shown in Figure 9.

ISSN: 2715-6427

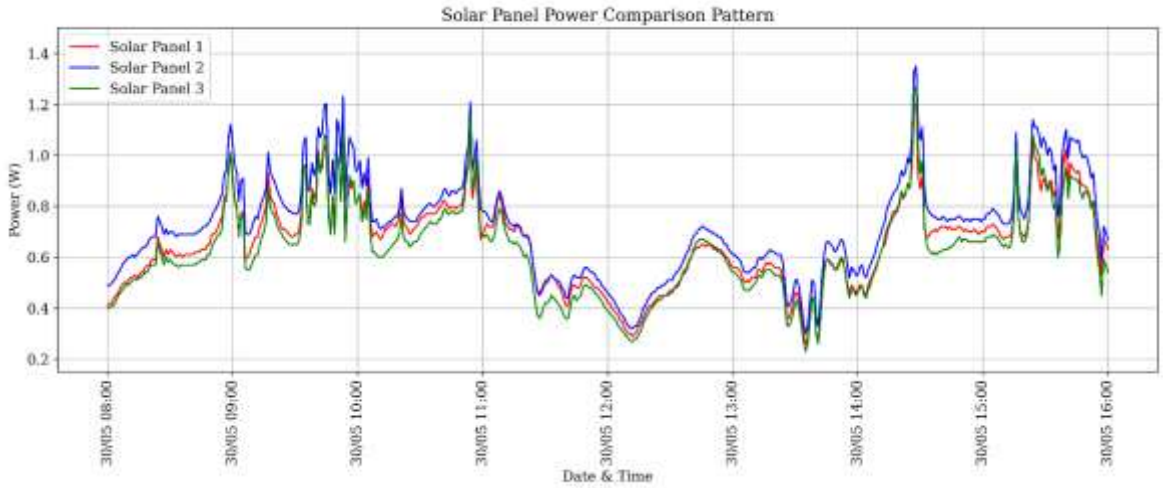

Figure 9. Power output profiles of three solar panels in day one

3.3.2 Day two

During the second test, which was conducted under more dynamic weather conditions, the power output profile exhibited greater fluctuations, particularly between 10:00 and 12:00 WIB, likely due to intermittent cloud cover. Solar Panel 2 again delivered the highest average power, while Solar Panels 1 and 3 followed closely with similar performance patterns. The system recorded peak values slightly above 1.3 W and occasional dips below 0.2 W, effectively capturing transient changes in irradiance with high accuracy. Despite the more variable environmental conditions, the system maintained stable operation, successfully collecting complete datasets and confirming its effectiveness for real-time monitoring and comparative performance analysis across multiple PV channels, as shown in Figure 10.

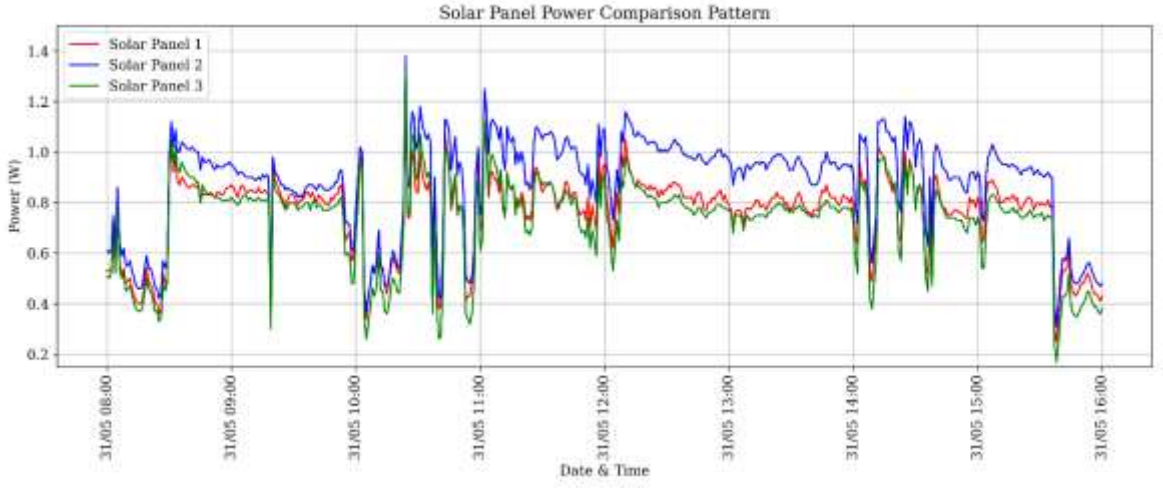

Figure 10. Power output profiles of three solar panels in day two

3.4 Data visualization

The system employs the ThingSpeak IoT platform to visualize real-time power data from each solar panel. Individual charts present the power output trends of the three panels, allowing users to easily monitor and compare their performance. By focusing exclusively on power, the interface becomes simpler to interpret and more accessible to non-technical users. The web-based dashboard offers immediate feedback on panel behavior, supports remote access through a browser, and enhances the overall usability of the monitoring system, as shown in Figure 11.

Figure 11. Dashboard Thingspeak

3.5 Discussion

The INA219 current–voltage sensor was selected for its high-resolution digital output, low power consumption, and I²C communication compatibility, making it well-suited for real-time power monitoring in photovoltaic applications. In this study, the sensor modules were calibrated against a digital multimeter prior to deployment, yielding an average voltage error of less than 1% and current RMSE values below 7 mA. Additionally, the coefficient of determination (R^2) for all three sensor modules exceeded 0.9998, indicating a very high level of linear correlation between the sensor readings and reference measurements. These results are consistent with prior work by Kusuma et al. [17], who reported voltage accuracy of 99.87% and current accuracy of 91.43%, with RMSE values of 0.0146 V and 227.65 mA, respectively, when using INA219 for battery monitoring. The high level of accuracy across both studies validates the sensor's reliability in outdoor monitoring environments.

Following sensor calibration, the system was subjected to two consecutive 8-hour test sessions. During each session, it successfully recorded and transmitted 481 data points per day without any interruption. This 100% success rate validates the reliability of both the microSD card storage and Wi-Fi-based cloud transmission components. The one minute data sampling interval was consistently maintained, ensuring stable temporal resolution for continuous monitoring applications. These findings confirm that the system's hardware and software architecture is suitable for long-term deployment in real-world solar monitoring scenarios.

Variations in power output across the three panels were observed during testing. These differences are likely attributed to environmental and physical factors, including partial shading, panel orientation, surface cleanliness, and intrinsic efficiency differences [14, 15]. Such deviations highlight the importance of per-panel monitoring, as aggregate measurements may obscure localized anomalies that could negatively affect overall system performance. The use of the INA219 current–voltage sensor further supports accurate per-channel analysis, as it provides high-resolution digital output with I²C communication. Compared to other sensors like the ACS712, the INA219 demonstrates superior performance in detecting current fluctuations and maintaining stability during surge conditions, as evidenced in prior implementations for motor control systems [21].

The ThingSpeak IoT platform was utilized in this study as the primary medium for real-time data visualization and cloud storage. This platform offers a user-friendly interface and supports HTTP-based API communication, allowing seamless integration with the ESP32 microcontroller for scheduled data uploads at one-minute intervals. Throughout the testing period, the system achieved a 100% transmission success rate with no packet loss, enabling continuous remote monitoring of panel performance. These findings align with Ibrahim et al. [22], highlighting ThingSpeak's capability to facilitate reliable data tracking and trend visualization. This validates the platform as a practical solution for IoT applications that demand affordability and ease of access.

Despite its strong operational performance, the current system is limited to electrical measurements and does not include environmental parameters such as surface temperature or solar irradiance. The absence of

such data restricts deeper analysis, particularly when assessing efficiency losses under dynamic outdoor conditions. Since photovoltaic modules are known to exhibit reduced performance at elevated temperatures, the lack of thermal context limits the interpretation of output variability, especially under high solar exposure. Future work will focus on integrating additional environmental sensors, including DS18B20 sensor to capture panel surface temperature.

4. CONCLUSION

A multi-channel power data acquisition system for solar panel monitoring was successfully designed, calibrated, and tested using ESP32 microcontrollers and INA219 sensors. The INA219 sensors achieved measurement accuracy exceeding 98%, with maximum errors of 1.02% for current and 0.43% for voltage. The system provided reliable real-time power monitoring of individual solar panels, maintaining high measurement accuracy and consistent data transmission over extended durations. An 8-hour field test revealed performance variations among panels and demonstrated the system's capability to identify local inefficiencies. Throughout the test, all data were 100% transmitted successfully to the ThingSpeak platform without packet loss. Integration with ThingSpeak enabled user-friendly data visualization, thereby improving practical usability. The system represents a scalable and cost-effective solution for photovoltaic monitoring, with opportunities for further enhancement through the integration of thermal parameters and assessment of cooling mechanisms.

ACKNOWLEDGEMENTS

The authors gratefully acknowledge the Renewable Energy Laboratory of Universitas Maritim Raja Ali Haji (UMRAH) for facility and support. Appreciation is also extended to colleagues and students for their assistance during hardware assembly and field testing.

REFERENCES

[1] A. Mehmood, J. Ren, and L. Zhang, "Achieving Energy Sustainability by Using Solar PV : System Modelling And Comprehensive Techno-economic-environmental Analysis," *Energy Strateg. Rev.*, vol. 2, no. 1, pp. 1–14, 2023, doi: 10.1016/j.esr.2023.101126.

[2] M. Deveci, U. Cali, and D. Pamucar, "Evaluation of Criteria For Site Selection of Solar Photovoltaic (PV) Projects Using Fuzzy Logarithmic Additive Estimation of Weight Coefficients," *Energy Reports*, vol. 7, no. 2, pp. 8805–8824, 2021, doi: 10.1016/j.egyr.2021.10.104.

[3] Q. Cao, C. Shen, and M. Jia, "A Fault Detection Scheme for PV Modules in Large Scale PV Stations With Complex Installation Conditions," *Energy*, vol. 2, no. 4, pp. 1–6, 2021, doi: 10.48550/arXiv.2105.08943.

[4] Ovie Vincent Erhueh, Chukwuebuka Nwakile, Enobong Hanson, Andrew Emuobosa Esiri, and Tari Elete, "Enhancing energy production through remote monitoring: Lessons for the future of energy infrastructure," *Eng. Sci. Technol. J.*, vol. 5, no. 10, pp. 3014–3053, 2024, doi: 10.51594/estj.v5i10.1671.

[5] D. Benavides, P. Arévalo, A. C. Ortega, F. Sánchez-Sutil, and E. Villa-Ávila, "Energy Management Model for a Remote Microgrid Based on Demand-Side Energy Control," *Energies*, vol. 17, no. 1, 2024, doi: 10.3390/en17010170.

[6] P. D. C. S. Patil, M. S. P. Sathe, A. A. Patil, A. N. Mahajan, and S. S. Chavhan, "Future of Agro Industry with Advance Monitoring using Thingspeak," *Int. J. Res. Appl. Sci. Eng. Technol.*, vol. 11, no. 6, pp. 2058–2062, 2023, doi: 10.22214/ijraset.2023.53984.

[7] B. E. Demir, "A New Low-Cost Internet of Things-Based Monitoring System Design for Stand-Alone Solar Photovoltaic Plant and Power Estimation," *Appl. Sci.*, vol. 3, no. 2, pp. 1–12, 2023, doi: doi.org/10.3390/app132413072.

[8] A. Rivai and N. A. Rahim, "A Low-cost Photovoltaic (PV) Array Monitoring System," *Clean Energy Technol.*, vol. 3, no. 2, pp. 169–174, 2016, doi: 10.1109/CEAT.2013.6775620.

[9] T. Sutikno, H. S. Purnama, A. Pamungkas, A. Fadlil, I. M. Alsofyani, and M. H. Jopri, "Internet of things-based photovoltaics parameter monitoring system using NodeMCU ESP8266," *Int. J. Electr. Comput. Eng.*, vol. 11, no. 6, pp. 5578–5587, 2021, doi: 10.11591/ijece.v11i6.pp5578-5587.

[10] S. Triwijaya, D. Aulia Feriando, R. Feriza, and Y. Don, "Realtime And Centralized Solar Panel Online Monitoring System Design Using Thingspeak," *J. Railw. Transp. Technol.*, vol. 2, no. 1, pp. 1–9, 2023, doi: 10.37367/jrtt.v2i1.18.

[11] Y. Sheikh, M. Jasim, M. Qasim, A. Qaisieh, M. O. Hamdan, and F. Abed, "Enhancing PV Solar Panel Efficiency Through Integration with a Passive Multi-layered PCMs Cooling Cystem: A Numerical Study," *Int. J. Thermofluids*, vol. 4, no. 2, pp. 1–17, 2024, doi: 10.1016/j.ijft.2024.100748.

[12] F. Y. Prasetyawati, D. Harjunowibowo, A. Fauzi, B. Utomo, and D. Harmanto, "Calibration and Validation of INA219 as Sensor Power Monitoring System using Linear Regression," *AIUB J. Sci. Eng.*, vol. 22, no. 3, pp. 240–249, 2023, doi: 10.53799/AJSE.V22I3.595.

[13] Z. P. Muqorrobin, A. Nawawi, A. Aris Ardani, S. Putra Setia, and R. Rahmadian, "Off-Grid Solar System Monitoring based on ESP-32 and INA219 In Pesanggrahan Gordomulyo," *Vokasi Unesa Bull. Eng. Technol. Appl. Sci.*, vol. 1, no. 2, pp. 26–37, 2024, doi: 10.26740/vubeta.v1i2.34859.

[14] F. Serepas, I. Papias, K. Christakis, N. Dimitropoulos, and V. Marinakis, "Lightweight Embedded IoT Gateway for Smart Homes Based on an ESP32 Microcontroller," *Computers*, vol. 14, no. 9, pp. 1–19, 2025, doi: 10.3390/computers14090391.

[15] J. S. Botero-Valencia, M. Mejia-Herrera, and J. M. Pearce, "Low Cost Climate Station for Smart Agriculture Applications with

Photovoltaic Energy and Wireless Communication," *HardwareX*, vol. 11, no. 2, pp. 1–21, 2022, doi: 10.1016/j.ohx.2022.e00296.

[16] M. Cassel, O. Navratil, F. Perret, and H. Piégay, "The e-RFIDuino: An Arduino-based RFID Environmental Station to Monitor Mobile Tags," *HardwareX*, vol. 10, no. 2, pp. 1–13, 2021, doi: 10.1016/j.ohx.2021.e00210.

[17] H. A. Kusuma, R. Ariandhi, S. Refly, and S. Nugraha, "Development Arduino Data Logger using INA219 Sensor for Battery Capacity Monitoring," *J. Tek. Elektro dan Komputasi*, vol. 5, no. 1, pp. 9–15, 2023, doi: 10.32528/elkom.v5i1.8352.

[18] W. Mendenhall, R. J. Beaver, and B. M. Beaver, *Introduction to Probability and Statistics*, 13th ed. Canada: Brooks/Cole, Cengage Learning, 2013.

[19] C. M. Nkinyam, C. O. Ujah, K. C. Nnakwo, O. Ezeudu, D. V. V. Kallon, and I. Ike-Eze C. Ezema, "Design and Implementation of a Waterless Solar Panel Cleaning System," *Unconv. Resour.*, vol. 5, no. 3, pp. 1–11, 2024, doi: 10.1016/j.uncres.2024.100131.

[20] S. Ganesan, P. W. David, P. K. Balachandran, and I. Colak, "Power Enhancement in PV Arrays Under Partial Shaded Conditions with Different Array Configuration," *Heliyon*, vol. 10, no. 2, pp. 2–18, 2024, doi: 10.1016/j.heliyon.2024.e23992.

[21] A. Maarif and N. R. Setiawan, "Control of DC Motor Using Integral State Feedback and Comparison With PID: Simulation and Arduino Implementation," *J. Robot. Control*, vol. 2, no. 5, pp. 456–461, 2021, doi: 10.18196/jrc.25122.

[22] A. O. Ibrahim *et al.*, "Indoor Condition Monitoring Using Thingspeak To Minimize Occupant ' s Health Challenges," vol. 27, no. 3, 2024.